



## OPEN

SUBJECT AREAS:  
NANOSENSORS  
ELECTROCHEMISTRY  
SENSORS  
BIOSENSORSReceived  
5 August 2014Accepted  
14 October 2014Published  
4 November 2014Correspondence and  
requests for materials  
should be addressed to  
Y.-Y.S. (yysong@mail.  
neu.edu.cn)Development of Amperometric Glucose  
Biosensor Based on Prussian Blue  
Functionlized TiO<sub>2</sub> Nanotube ArraysZhi-Da Gao<sup>1,2</sup>, Yongfang Qu<sup>1</sup>, Tongtong Li<sup>1</sup>, Nabeen K. Shrestha<sup>3</sup> & Yan-Yan Song<sup>1</sup><sup>1</sup>College of Sciences, Northeastern University, Shenyang 110004, China, <sup>2</sup>National Laboratory of Solid State Microstructures, Nanjing University, Nanjing 210093, China, <sup>3</sup>Department of Chemistry, Hanyang University, Haengdang-dong 17, Sungdong-gu, Seoul 133-791, South Korea.

Amperometric biosensors consisting of oxidase and peroxidase have attracted great attention because of their wide application. The current work demonstrates a novel approach to construct an enzymatic biosensor based on TiO<sub>2</sub> nanotube arrays (TiNTs) as a supporting electrode on which Prussian Blue (PB)-an “artificial enzyme peroxidase” and enzyme glucose oxidase (GOx) have been immobilized. For this, PB nanocrystals are deposited onto the nanotube wall photocatalytically using the intrinsic photocatalytic property of TiO<sub>2</sub>, and the GOx/AuNPs nanobiocomposites are subsequently immobilized into the nanotubes via the electrodeposition of polymer. The resulting electrode exhibits a fast response, wide linear range, and good stability for glucose sensing. The sensitivity of the sensor is as high as 248 mA M<sup>-1</sup> cm<sup>-2</sup>, and the detection limit is about 3.2 μM. These findings demonstrate a promising strategy to integrate enzymes and TiNTs, which could provide an analytical access to a large group of enzymes for bioelectrochemical applications including biosensors and biofuel cells.

Fast, sensitive and reliable glucose biosensor has attracted considerable attention since Clark proposed the first enzyme glucose biosensor in 1962<sup>1</sup>. While fulfilling the requirements on high specificity and sensitivity, it is highly desirable that these sensors should allow rapid high-throughput analysis. However, the oxidase-based amperometric biosensors are sensitive to the variable oxygen concentrations present in the solution. In addition, a relatively high potential is needed to be applied to efficiently oxidize hydrogen peroxide for this type of biosensors. This could lead to the electrochemical oxidation of ascorbic acid and uric acid (which are always found in the blood sample), and hence causes interfering signals in the amperometric measurement. To overcome these problems, peroxidase (i.e. HRP) is usually employed to cooperate with glucose oxidase<sup>2-4</sup>. The as-formed oxidase/peroxidase bienzyme systems allow the detection principle to switch from an electrochemical oxidation to a reduction process that takes place at much lower potentials, and thereby improves the selectivity of the biosensors considerably. On the other hand, redox mediators are also frequently employed in bienzyme sensors as an electronic communicator between HRP and oxidase. However, the competition between reactions involving oxygen and the mediator are usually observed<sup>5,6</sup>.

Owing to the high activity and selectivity toward the reduction of H<sub>2</sub>O<sub>2</sub> and O<sub>2</sub>, Prussian blue (PB), i.e., Fe<sub>4</sub>[Fe(CN)<sub>6</sub>]<sub>3</sub>, has been employed extensively as an “artificial enzyme peroxidase” in the construction of electrochemical amperometric biosensors<sup>7,8</sup>. Xia and coworkers demonstrated that PB could deposit directly on semiconductor (for example, TiO<sub>2</sub> and Si) surfaces via photocatalytic deposition or galvanic displacement from a ferricyanide or ferric ions containing solution<sup>9,10</sup>. Based on the photocatalytic property and their unique architectural morphology<sup>11,12</sup>, anodically grown TiO<sub>2</sub> nanotube arrays (TiNTs) can be a promising supporting electrode material in construction of electrochemical biosensors because the anodic TiNTs are grown directly on a titanium-metal substrate. Therefore, the as-formed TiNTs are directly back-contacted, and thus provide a beneficial feature to use TiNTs directly as electrode materials. Specially, considering the distinct tubular features, such as regular arrays perpendicular to the substrate surface, large surface area, high pore volume, good mechanical strength and biocompatibility, TiNTs are becoming more attractive and promising material in the construction of biosensing platforms<sup>13-17</sup>. However, the widespread use of TiNTs is limited due to their poor electronic conductivity<sup>18</sup>.

In this context, we report the preparation of a mediator-free biosensing system based on PB and GOx modified TiNTs nanocomposites. To the best of our knowledge, no attempt has been made on combination of TiNTs and



PB for the construction of enzymatic amperometric glucose sensor. This could be due to the poor electrochemical conductivity of TiNTs, instable operational ability and slight dissolubility of PB. In the present study, the negatively charged AuNPs are attached to the tube surfaces and walls via PDDA bridges. It should be noted that even after modification of TiNTs, the AuNPs/TiNTs nanocomposite still maintains the excellent photocatalytic activity of TiO<sub>2</sub>. Therefore, the deposition of PB nanoparticles on the AuNPs/TiNTs is achieved by applying the photocatalytic reaction in an acidic ferricyanide solution. The tube wall is subsequently modified with a layer of polymeric matrix of poly-(1,2-diaminobenzene) (pDAB) by electrochemical polymerization to integrate PB and GOx into the nanotubes, which on the other hand also avoids the leaching of PB. The resulted enzymatic electrode shows stable and selective responses towards glucose sensing. Due to the synergistic effect of the good electrical conductivity of AuNPs and the high electrocatalytic ability of PB, an improved sensitivity response is achieved.

## Results

The construction of enzymatic electrode based on TiO<sub>2</sub> nanotube arrays is briefly illustrated in Fig. 1A. The electrochemical activity and the stability of the PB modified AuNPs/TiNT electrode was investigated using CV. Fig. 1B shows typical CVs of the PB modified AuNPs/TiNT electrode in a PBS solution. The couple of reversible redox peaks located at  $\sim -0.40$  V originated from the transformation process between Prussian blue (PB) and Prussian white (PW) can be observed in the voltammograms. However, the as-formed PB modified electrode shows non-ignorable decrease in anodic and cathodic peak currents by 15  $\mu$ A and 52  $\mu$ A, respectively after scanning for 30 cycles. The observed decrease in anodic and cathodic peak currents can be attributed to the dissolution of PB in the electrolyte during the repeated electrochemical scanning. Fig. 1C exhibits the CVs from PB/AuNPs/TiNT after covered a layer of poly(1,2-diaminobenzene) (pDAB) by electrochemical scanning between

$-0.25$  and  $1.0$  V for 5 cycles. The decrease in the anodic and cathodic peak currents after 30 cycles is only by 3  $\mu$ A and 15  $\mu$ A, respectively which are considerably less than before deposition of pDAB film (Fig. 1B).

GOx molecules were immobilized into the nanotubular electrodes with the electrochemical deposition of pDAB. As shown in Fig. 2A, due to the presence of nonconducting polymer on electrode surface, the electron transfer between the electrode and the electrolyte is hindered. Consequently, the anodic currents decrease accordingly with the polymerization of 1,2-DAB on every CV scanning. This tendency is consistent with the previous reports<sup>19</sup>. Fig. 2B exhibits the FTIR spectra of the PB/AuNP/TiNTs (curve i), pDAB-PB/Au/TiNTs (curve ii), and (GOx-pDAB)-PB/AuNP/TiNTs (curve iii) electrodes. The absorption band at  $2089\text{ cm}^{-1}$  in PB/AuNP/TiNTs spectrum is a common characteristic of PB, corresponding to the stretching vibration of CN group. After depositing pDAB film onto PB/AuNP/TiNTs (curve ii), the bands at  $3400$  and  $3185\text{ cm}^{-1}$  appear, which can be assigned to the stretching mode of N–H and NH<sub>2</sub> groups present in the polymer<sup>20</sup>. Besides, the presence of the bands at  $1632$  and  $1503\text{ cm}^{-1}$  are belonged to the C=C stretching vibrations, and the band at  $748\text{ cm}^{-1}$  is originated from the out of plane C–H bending vibration of the benzoid rings. After introducing enzyme molecules into the nanotubes with pDAB (curve iii), two absorption bands are observed at around  $1646\text{ cm}^{-1}$  (amide I) and  $1520\text{ cm}^{-1}$  (amide II), respectively, which can be assigned to the C–O stretching mode from the carboxylic acid groups of the enzyme molecules, and a combination of the N–H bending and C–N stretching of the amide plane in the backbone of protein, respectively. The existing amide I and II bands confirms the successful immobilization of GOx into the nanotubular structure by the formation of polymeric matrix.

To investigate the effect of pDAB thickness on electrochemical response of the resulted biosensor, the electrochemical behaviours of the (GOx/pDAB)-PB/AuNP/TiNTs electrodes prepared by different

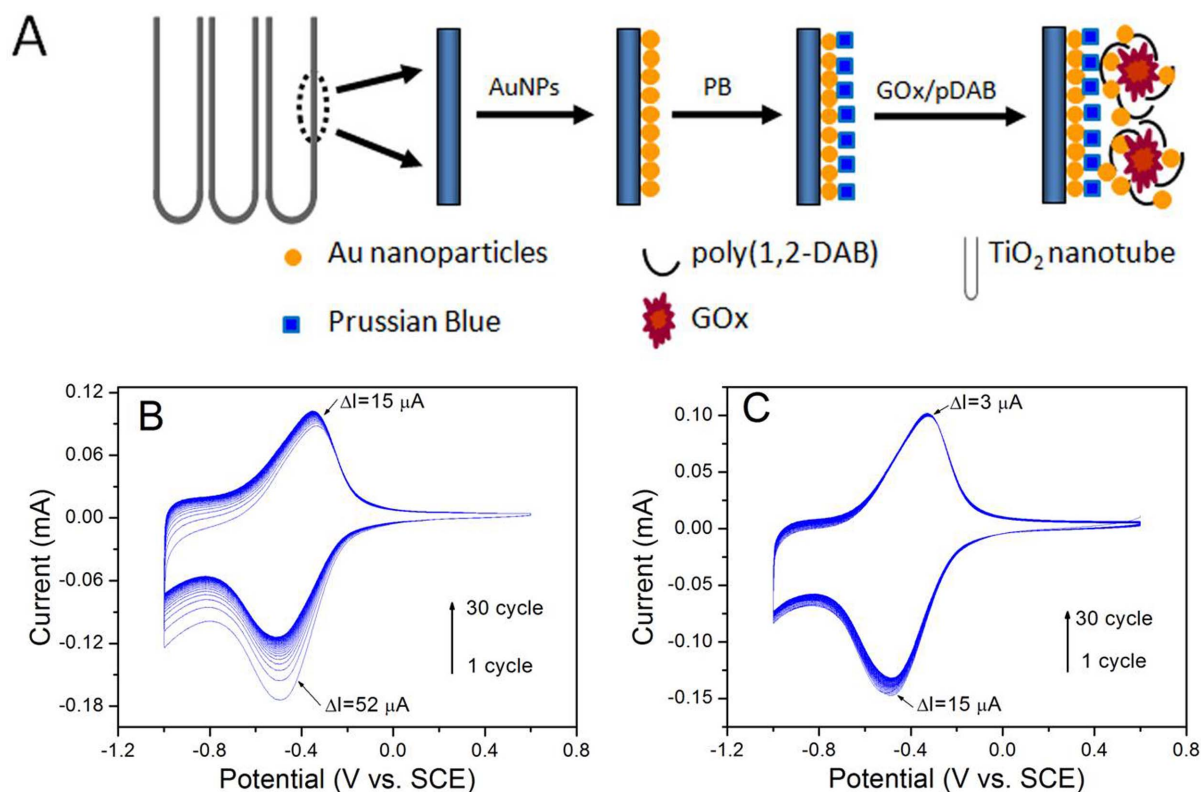


**Figure 1** | (A) Schematic illustration for preparing “bienzyme” electrode based on TiO<sub>2</sub> nanotube arrays. Cyclic voltammograms of the (B) PB/AuNP/TiNT and (C) pDAB-PB/AuNP/TiNTs nanocomposite electrode in air-saturated 0.01 M PBS (pH 6.0) at a scan rate of 50 mV s<sup>-1</sup>.

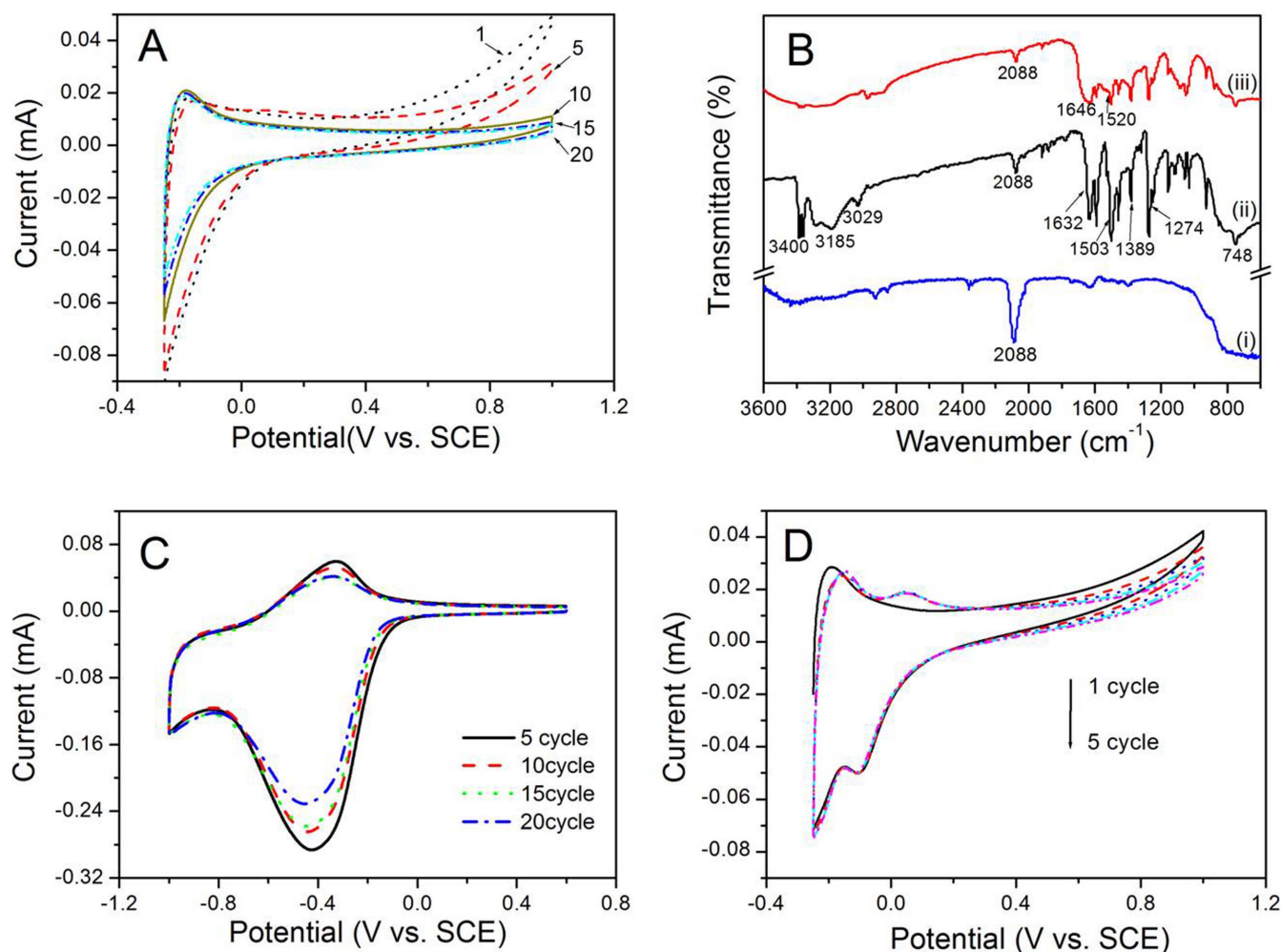


**Figure 2** | (A) Cyclic voltammograms of poly-(1,2-DAB) electrodeposition on PB/AuNP/TiNTs electrode. (B) FT-IR spectra of PB/AuNP/TiNTs (curve i), pDAB-PB/AuNP/TiNTs (curve ii) and (GOx-pDAB)-PB/AuNP/TiNTs sample (curve iii). (C) Cyclic voltammograms of the (GOx-pDAB)-PB/AuNP/TiNTs electrodes in a PBS solution with 10 mM glucose. The electrodes were prepared by 5, 10, 15 and 20 CV electropolymerization cycles as illustrated in Fig. 2A. (D) Cyclic voltammograms of electrodeposition of GOx and AuNPs onto the PB/AuNP/TiNTs electrode via the electropolymerization of 1,2-DAB. Numerals indicated the numbers of electropolymerization cycles. Scan rate: 50 mV s<sup>-1</sup>.

number of CV cycles (used for polymerization) were studied in the presence of 10 mM glucose. As evident in Fig. 2C, the as-formed biosensors demonstrate the best electrocatalytic activity towards glucose detection when the polymeric film was deposited by 5 polymerization cycles. Therefore, the number of electropolymerization cycles for the further investigation was optimized to 5 cycles. Fig. 2D represents the progress on electropolymerization process to prepare (GOx/Au/pDAB)-PB/AuNP/TiNTs electrode.

The SEM images in Fig. 3A show the morphology of the as-prepared (GOx/pDAB)-PB/AuNP/TiNTs electrode. Clearly, AuNPs and PB nanocrystals can be observed on the tube entrance and wall. However, as the polymer film is quite thin, it is hard to distinguish pDAB film in the SEM image. Fig. 3B exhibits the morphology of (GOx/Au/pDAB)-PB/AuNP/TiNTs electrode prepared in the presence of AuNPs. Compared to the (GOx/pDAB)-PB/AuNP/TiNTs electrode (Fig. 3A), larger number of AuNPs can be observed on the tube surface of the (GOx/Au/pDAB)-PB/AuNP/TiNTs electrode (Fig. 3B). To gain information on the composition, energy-dispersive X-ray spectroscopy (EDX) of the two electrodes were acquired. The EDX analysis shows that the Au content on the (GOx/Au/pDAB)-PB/AuNP/TiNTs electrode (0.18 atm%, Fig. 3D) is much higher than that on the (GOx/pDAB)-PB/AuNP/TiNTs (0.10 atm%, Fig. 3C). These results demonstrate that more AuNPs are deposited on the

(GOx/Au/pDAB)-PB/AuNP/TiNTs electrode, and parts of the AuNPs are immobilized during 1,2-DAB polymerization process.

To gain a better understanding of the influence of adding AuNPs into polymer matrix on the electrochemical responses of biosensor, the electrochemical activities of the as-prepared enzymatic electrodes towards glucose sensing were compared. As evident in Fig. 4A, the (GOx/pDAB)-PB/AuNP/TiNTs and (GOx/Au/pDAB)-PB/AuNP/TiNTs electrodes exhibit the similar (curve a and c) currents in 0.01 M PBS solution (pH 6.0, containing 0.1 M KCl) at scan rate of 50 mV s<sup>-1</sup>. Upon addition of 10 mM glucose into the PBS solution, the rapid increases in the cathodic currents appear as a result of the reduction of hydrogen peroxide (H<sub>2</sub>O<sub>2</sub>) produced from the enzymatic reaction. The (GOx/Au/pDAB)-PB/AuNP/TiNTs based electrode (curve d) exhibits a higher response current to 10 mM glucose than by the (GOx/pDAB)-PB/AuNP/TiNTs electrode (curve b), suggesting the (GOx/Au/pDAB)-PB/AuNP/TiNTs electrode has a better biocatalytic activity for glucose.

The effect of pH was evaluated at different pH values in 0.01 M PBS (containing 0.1 M KCl) at 25 °C. As shown in Fig. 4B, both the (GOx/pDAB)-PB/AuNP/TiNTs electrode (curve a) and (GOx/Au/pDAB)-PB/AuNP/TiNTs electrode (curve b) show the highest response at pH 6.0, which is deviated from the optimum pH observed for free GO<sup>21</sup>. The possible reason could be the presence of hydroxyl

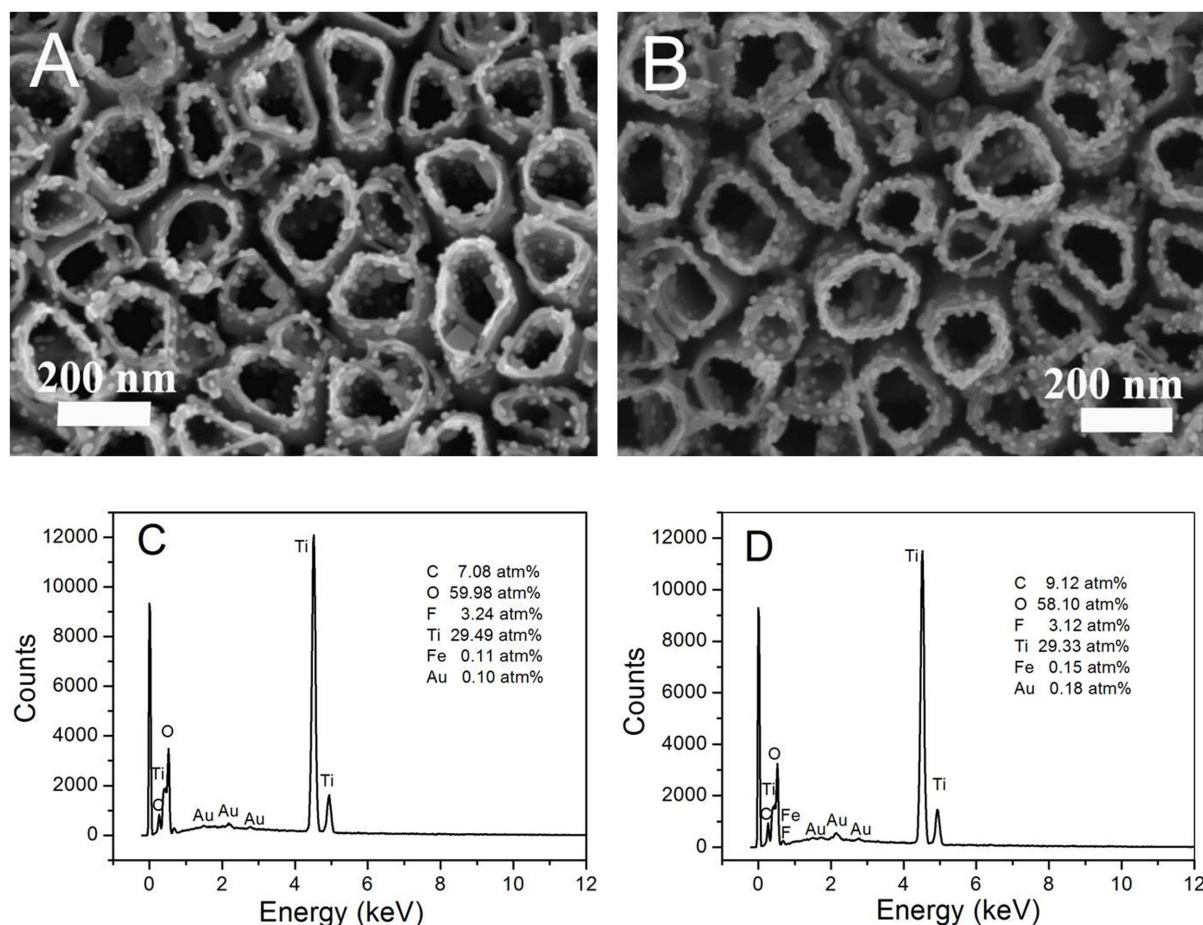


**Figure 3** | SEM images of the as-prepared (A) (GOx/pDAB)-PB/AuNP/TiNTs and (B) (GOx/Au/pDAB)-PB/AuNP/TiNTs samples; EDX spectra of the (C) (GOx/pDAB)-PB/AuNP/TiNTs and (D) (GOx/Au/pDAB)-PB/AuNP/TiNTs samples.

ions as the products of  $\text{H}_2\text{O}_2$  reduction at the electrode surface. Hydroxyl ions are known to be able to break the Fe-CN-Fe bonds, and hence the dissolution of PB takes place<sup>22</sup>. As shown in inset of Fig. 4B, the pH dependencies of the peak currents of PB/AuNPs/TiNTs in various pH media from 5.5 to 8.5 buffered by 10 mM phosphate is investigated. The cathodic peak currents are also decreased sharply as the pH greater than 6.0. This is in good agreement with the fact that PB exhibits tendency to decompose under alkaline conditions. Taking several factors into consideration, such as enzymatic activity and PB stability, the electrolyte was then buffered at pH of 6.0 in this study.

The effect of glucose concentration was measured by adding different concentrations of glucose to the PBS electrolyte under being investigated. Since the electrochemical signal is resulted from the reduction of PB on the sample, the differences in cathodic current is observed in amperometric measurement. Fig. 4C and 4D show the chronoamperometric response of the as-prepared electrodes on the successive increment of glucose to the PBS under stirring at an applied potential of  $-0.35$  V. For the (GOx/pDAB)-PB/AuNP/TiNTs based electrode (Fig. 4C), a linear increase in reduction current with the increase in glucose concentration in the range of 0.03–0.30 mM with a detection limit of  $6.9$   $\mu\text{M}$  (estimated from 3 times the standard deviation of the blank) was observed. The regression equation of the linear part of the curve was  $y = -49.37x + 0.85$ , where  $y$  represents the current in  $\mu\text{A}$  and  $x$  the glucose concentration in mM; the  $R^2$  was 0.986. The sensitivity was  $30.6$   $\text{mA M}^{-1} \text{cm}^{-2}$ . After introducing AuNPs into polymer matrix (Fig. 4D), the resulted (GOx/Au/pDAB)-PB/AuNP/TiNTs electrode exhibits a improved sensing ability. The linear range of such biosensor for the determination of glucose was found to be 0.01 to 0.70 mM with a detection

limit of  $3.2$   $\mu\text{M}$ . The linear regression equation was:  $y = -106.14x - 1.32$ , where  $y$  represents the current in  $\mu\text{A}$  and  $x$  the glucose concentration in mM; the  $R^2$  was 0.990. The sensitivity of such biosensor is  $248.0$   $\text{mA M}^{-1} \text{cm}^{-2}$ .

The selectivity of the present electrodes was examined by studying the effects of electroactive species on the determination of 1 mM glucose. As shown in Fig. 5, the (GOx/pDAB)-PB/AuNP/TiNTs and (GOx/Au/pDAB)-PB/AuNP/TiNTs electrodes show a very rapid response to glucose- the current reaches 95% of the maximum current within 1 s after glucose addition. It is very important to note that there is practically no interference in the response measurement of AP, AA and UA for both electrodes.

The ultimate goal on the development of a biosensor is for its practical application in monitoring serum chemistry profile of human beings. Therefore, it is noteworthy to investigate the proposed enzymatic biosensor for the measurement of glucose in human serum samples. For such measurement, the blood samples were diluted 10 times with PBS and the diluted samples were analyzed by the prepared biosensors at a potential of  $-0.35$  V. The assay results determined by the as-prepared electrodes are tabulated in table 1. It can be seen that the values measured by both of the bienzyme systems (average of three determinations) are very close to the results obtained by the clinic determination.

## Discussion

Basically, TiNTs are negatively charged in a neutral solution<sup>23</sup>. Therefore, cationic polyelectrolyte PDDA can wrap TiNTs via electrostatic interaction<sup>24</sup>. After the formation of positively charged PDDA-modified TiNTs, the negatively charged AuNPs are attached to the tube surfaces and walls through the PDDA bridges. The

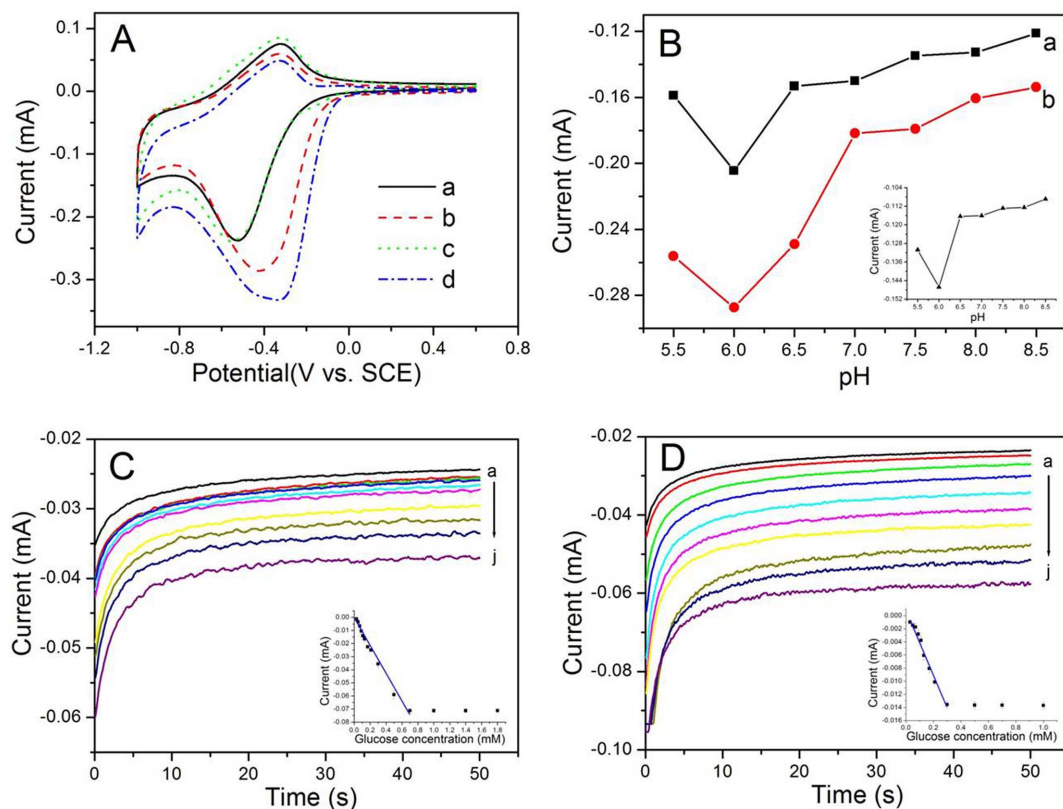


**Figure 4** | (A) Cyclic voltammograms of the (GOx/pDAB)-PB/AuNP/TiNTs based electrode (curve a and b), and (GOx/Au/pDAB)-PB/AuNP/TiNTs based electrode (curve c and d) in absence (curve a and c) and presence (curve b and d) of 10 mM glucose in PBS (pH 6.0). (B) Effect of pH on the response of the (GOx/pDAB)-PB/AuNP/TiNTs (curve a) and (GOx/Au/pDAB)-PB/AuNP/TiNTs (curve b) based electrode to 10 mM glucose; inset shows the effect of pH on reduction peak current of the PB/AuNP/TiNTs electrode. Amperometric response of (C) (GOx/pDAB)-PB/AuNP/TiNTs electrode and (D) (GOx/Au/pDAB)-PB/AuNP/TiNTs electrode (a) in the absence and (b–j) successive addition of glucose at  $-0.35$  V; inset shows the linear calibration plot.

attached AuNPs can largely improve the electronic conductivity as well as the photocatalytic activity of the TiNTs<sup>13</sup>. Under UV light irradiation, the photoinduced reaction deposits PB nanocubes on the tube wall of AuNP/TiNTs nanocomposite<sup>9</sup>. To suppress the dissolution of PB and thereby to improve the stability of PB modified

nanotubular electrode, thin film of poly(1,2-diaminobenzene) (pDAB) (which is a nonconducting polymeric film) was deposited on the top of the PB/AuNPs/TiNT electrode. Compared to the PB/AuNPs/TiNTs electrode (Fig. 1A), a significant improvement in its electrochemical stability is achieved for the resulted pDAB-PB/AuNPs/TiNTs electrode (Fig. 1B). This finding clearly shows that the deposition of thin film of pDAB is an effective way to inhibit the leakage of PB into the surrounding solution, and hence the increased electrochemical stability of the PB-modified electrodes is achieved.

Due to the ability of AuNPs to bind biomolecules, the enzyme molecules absorb onto the surface of AuNPs during mixing. When GOx molecules and AuNPs are introduced into pDAB matrix synchronously, as shown in Fig. 2D, it is noticeable that a pair of quasi-reversible peaks appears from the first scan of the electropolymerization process. The newly-appeared anodic peak potential ( $E_{pa}$ ) and cathodic peak potential ( $E_{pc}$ ) are located at 0.048 and  $-0.108$  V, respectively. The presence of the new pair of redox peaks can be attributed to an electrochemical reaction of the entrapped GOx between GOx-FAD and GOx-FADH<sub>2</sub>, via the promotion of Au nanoparticles. Its midpoint redox potential is  $-0.023$  V at a scan rate of  $50$  mV s<sup>-1</sup>, which is more positive than the redox potential of FAD in the native enzyme (ca.  $-0.5$  V vs. SCE at pH 6). The positive shift of the peak potentials is presumably attributed to the presence of the PB/AuNP/TiNTs, which has effect on the redox reaction of the immobilized GOx.

GOx molecules catalyze the oxidation of glucose to gluconic acid in the presence of natural co-substrate O<sub>2</sub>, with production of H<sub>2</sub>O<sub>2</sub>. At negative potentials, the Prussian blue is reduced to Prussian white, which subsequently reduces H<sub>2</sub>O<sub>2</sub>, and in the process of

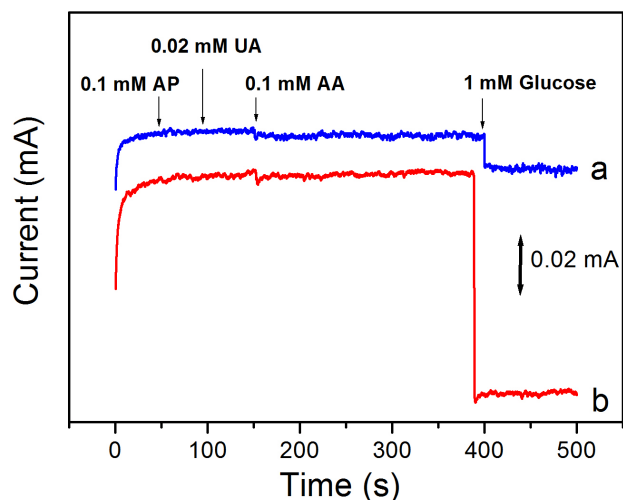


**Figure 5** | Amperometric response of the (GOx/pDAB)-PB/AuNP/TiNTs (curve a), and (GOx/Au/pDAB)-PB/AuNP/TiNTs (curve b) based electrodes for the addition of 0.1 mM AP, 0.02 mM UA, 0.1 M AA and 1.0 mM glucose at  $-0.35$  V to air-saturated PBS (pH 6.0). The equilibration time for addition of each interference is  $\sim 50$  s.



Table 1 | Determination of glucose in human serum samples

Sample no.	Hospital value	Determined by electrode 1 <sup>a</sup> mean $\pm$ SD (n=3)	Determined by electrode 2 <sup>b</sup> mean $\pm$ SD (n=3)
1	5.00	4.95 $\pm$ 0.055	5.03 $\pm$ 0.058
2	3.98	4.10 $\pm$ 0.089	4.05 $\pm$ 0.065

H<sub>2</sub>O<sub>2</sub> reduction, Prussian white is oxidized back to Prussian blue. As the resulted PB in turn is reduced electrochemically, determination of glucose in this sensing device can be achieved by measuring the current for the reduction of H<sub>2</sub>O<sub>2</sub>. In the absence of oxygen, the production of H<sub>2</sub>O<sub>2</sub> from dissolved oxygen was no longer available, and the reaction route based on electrochemical reduction of H<sub>2</sub>O<sub>2</sub> was blocked.

In Fig. 4A, despite the same top surface area and tube length of the TiNTs-based electrodes, the (GOx/Au/pDAB)-PB/AuNP/TiNTs based electrode (curve d) demonstrates a higher response current to glucose than by the (GOx/pDAB)-PB/AuNP/TiNTs electrode (curve b). In Fig. 4C and 4D, the (GOx/Au/pDAB)-PB/AuNP/TiNTs electrode displays a higher sensitivity, wider linear range, and lower limit of detection than the (GOx/pDAB)-PB/AuNP/TiNTs electrode. The enhanced response can be attributed to the excellent biocompatibility of Au nanoparticles, which provide a desirable microenvironment for adsorbed enzyme. Moreover, it is apparent that the sensitivity (248.0 mA M<sup>-1</sup> cm<sup>-2</sup>) of the resulted (GOx/Au/pDAB)-PB/AuNP/TiNTs electrode are comparable and even better than the recently reported results on GOx-PB decorated carbon nanomaterials such as carbon nanotubes (38.0 mA M<sup>-1</sup> cm<sup>-2</sup>)<sup>25</sup>, graphene (25.0 mA M<sup>-1</sup> cm<sup>-2</sup>)<sup>26</sup> and carbon nanofibers (6.0 mA M<sup>-1</sup> cm<sup>-2</sup>)<sup>27</sup>. Such an enhanced sensitivity arises from the large real surface area and nanoporous volume of the nanotubular structure of the electrode.

In medicine and animal physiology, "blood sugar" refers to glucose in the blood. However, many coexisting electroactive species [e.g., ascorbic acid (AA), uric acid (UA) and 4-acetaminophen (AP)] can also be easily oxidized at similar or even lower potentials, so that dramatically affects the selectivity of electrochemical biosensors. Normally, the blood-glucose level is maintained within the range 4–6 mM, which is much higher than that of AA and AP<sup>28</sup>. Using oxidase/Prussian Blue enzymatic systems, the detection principle switches from an electrochemical oxidation to a reduction process that takes place at much lower potentials. The high selectivity of the proposed electrodes can be attributed to the low operating potential and the systematic device architecture<sup>29,30</sup>. Furthermore, the poly(1,2-DAB) film acts as an effective perm-selective membrane for the electroactive interferences, and hence, the selectivity of the device is improved considerably.

The reproducibility and stability are two other important parameters for evaluating the performance of biosensors. The electrode-to-electrode reproducibility was examined among five different electrodes in the PBS solution containing 10 mM glucose. The relative standard deviation was calculated to be 3.2% and 2.8% for the (GOx/pDAB)-PB/AuNP/TiNTs and (GOx/Au/pDAB)-PB/AuNP/TiNTs electrodes, respectively. The stability was investigated over one and a half months by comparing the amperometric response of the as-prepared electrodes in presence of 10 mM glucose at regular intervals (every other day). For the first 30 days, both the electrodes retained more than 90% of their initial current response. After 45 days, 75% and 87% of the original response was exhibited by the (GOx/pDAB)-PB/AuNP/TiNTs and (GOx/Au/pDAB)-PB/AuNP/TiNTs electrodes, respectively showing the long term stability of the device. The improved stability of the (GOx/Au/pDAB)-PB/AuNP/TiNTs electrode is related to the excellent biocompatibility of the AuNPs for preserving the activity of the enzyme molecules. Nevertheless, some decrease in response signals after a long time

storing can be observed, which is probably due to the denaturation of the enzyme as a result of storing for a long time.

In summary, the present work demonstrates a novel approach for immobilizing GOx and PB to construct a sensitive and selective enzymatic glucose biosensor based on TiO<sub>2</sub> nanotube arrays as a supporting electrode. Due to the synergistic effect of the high electrocatalytic of PB and the good biocompatibility of AuNPs, the improved analytical performance of the enzymatic electrodes is achieved in term of short response time, good stability and no interference from the common electroactive species. Furthermore, owing to the large real surface area and nanoporous volume of the nanotubular electrode structure, the resulted electrode exhibits remarkably high sensitivity for the amperometric determination of glucose.

## Methods

**Materials.** Titanium foils (0.1 mm thick, 99.6% purity) were purchased from Baotai Metal Co. (Baotai, China). Glucose oxidase (GOx), β-D(+)-glucose, ascorbic acid (AA), uric acid (UA), p-acetamidophenol (AP), 1,2-diaminobenzene (1,2-DAB) and poly(diallyldimethylammonium chloride) (PDAA) were purchased from Sigma. Glycerol, hydrochloroauric acid (HAuCl<sub>4</sub>), ammonium fluoride (NH<sub>4</sub>F) and other chemicals were of analytical grade and used without further purification. All solutions were prepared with deionized (DI) water obtained from ultrapure water purification system (NW10VF, Heal Force Development Ltd.) with a resistivity of not less than 18 MΩ.

**Preparation of TiO<sub>2</sub> nanotube arrays.** Ti foils were first degreased by sonication in ethanol and DI water. Anodization was carried out for 3 h in glycerol/water (50 : 50) mix electrolyte containing 0.27 M NH<sub>4</sub>F at 30 V against a platinum foil serving as the counter electrode. The TiO<sub>2</sub> nanotube layers (TiNTs) thus formed were cleaned, dried, and then annealed at 450°C in air for 1 h to crystallize to an anatase phase.

**Preparation of PB modified AuNP/TiNTs samples.** To fabricate PB/AuNPs/TiNT samples, TiNTs were first decorated with a layer of PDAA by incubating the nanotube layers in 0.05% PDAA aqueous solution for 2 h at room temperature. After washing thoroughly with DI water, the PDAA-modified TiNTs were immersed into 10.0 mL of as-prepared colloidal AuNPs (~ 8 nm, 0.17 mg ml<sup>-1</sup>) at 4°C for 4 h. The resulted samples were placed into a quartz vessel containing 1 mM ferricyanide in the presence of 0.1 M KCl (pH 1.6), and subsequently photocatalytic deposition of PB was carried out by irradiating with a 300 W Hg lamp for 90 min.

**Preparation of poly(1,2-diaminobenzene) modified PB/AuNP/TiNTs samples.** To modify with poly(1,2-diaminobenzene) (pDAB), the PB/AuNP/TiNTs samples were placed in a deaerated PBS solution (0.01 M, pH 6.0) containing 0.1 M KCl and 10 mM 1,2-DAB. Electrochemical polymerization was carried out cyclic voltammetrically and scanning the potential between -0.25 and 1.0 V (vs. SCE) at a sweep rate of 50 mV s<sup>-1</sup> for 5–20 cycles. The resulted pDAB-PB/AuNP/TiNTs electrode was rinsed with the DI water.

**Preparation of enzymatic biosensors.** To fabricate enzymatic electrode viz. (GOx/pDAB)-PB/AuNP/TiNTs, 30 mg ml<sup>-1</sup> of GOx was dissolved in a deaerated PBS solution (pH 7.0) containing 10 mM 1,2-DAB. The gold nanoparticles doped enzymatic electrode ((GOx/Au/pDAB)-PB/AuNP/TiNTs) was prepared using the similar method. Briefly, GOx (30 mg ml<sup>-1</sup>) and Au colloids (0.17 mg ml<sup>-1</sup>) were completely mixed in a deaerated PBS solution (pH 7.0). Then, 1,2-DAB (10 mM) was added into the enzyme-AuNPs mixture and mixed it by stirring. The electrochemical polymerization of 1,2-DAB was carried out by scanning the applied potential in the range from -0.25 to 1.0 V at a sweep rate of 50 mV s<sup>-1</sup>. The resulted electrodes were thoroughly rinsed with DI water and stored at 4°C.

**Instruments.** The morphologies of TiNTs were characterized using a field-emission scanning electron microscope (FE-SEM, Hitachi S4800). IR spectra were recorded on a Nicolet-6700 Fourier IR spectrophotometer (Thermo, USA) and the electrochemical measurements were performed using a CHI660d electrochemical workstation (CH Instrument Co. China). The TiNT samples were contacted with a Cu back-plate (as working electrode), and pressed against an O-ring (8 mm in diameter) on the wall of a cell. Thus, the exposed area used for the electrochemical measurements was 0.5 cm<sup>2</sup>. A Pt foil and a saturated calomel electrode (SCE) were used as the counter and reference electrodes, respectively. Cyclic voltammograms (CVs) were measured at a sweep rate of 50 mV s<sup>-1</sup>, and amperometric measurements



were carried out at an applied potential of  $-0.35$  V with stirring using the phosphate-buffered saline (PBS, 0.01 M, containing 0.1 M KCl) as a supporting electrolyte.

- Clark, L. C. & Lyons, C. Electrode systems for continuous monitoring in cardiovascular surgery. *Ann. NY Acad. Sci.* **102**, 29–45 (1962).
- Tatsuma, T., Okawa, Y. & Watanabe, T. Enzyme monolayer- and bilayer-modified tin oxide electrodes for the determination of hydrogen peroxide and glucose. *Anal. Chem.* **61**, 2352–2355 (1989).
- Yao, Y. L. & Shiu, K. K. A mediator-free bienzyme amperometric biosensor based on horseradish peroxidase and glucose oxidase immobilized on carbon nanotube modified electrode. *Electroanalysis* **20**, 2090–2095 (2008).
- Mulchdani, A. & Chia, W. Bienzyme sensors based on poly(anilinomethylferrocene) modified electrodes. *Electroanalysis* **8**, 414–419 (1996).
- Gorton, L. *et al.* Amperometric biosensors based on an apparent direct electron transfer between electrodes and immobilized peroxidases. *Analyst* **117**, 1235–1241 (1992).
- Shobha Jeykumari, D. R. & Sriman Narayanan, S. Fabrication of bienzyme nanobiocomposite electrode using functionalized carbon nanotubes for biosensing applications. *Biosens. Bioelectro.* **23**, 1686–1693 (2008).
- Gorton, L. Carbon paste electrodes modified with enzymes, tissues, and cells. *Electroanalysis* **7**, 23–45 (1995).
- Karyakin, A. A. Prussian Blue and Its Analogues: Electrochemistry and Analytical Applications. *Electroanalysis* **13**, 813–819 (2001).
- Song, Y. Y., Zhang, K. & Xia, X. H. Photosynthesis and Characterization of Prussian Blue Nanocubes on Surfaces of  $\text{TiO}_2$  Colloids. *Appl. Phys. Lett.* **88**, 053112 (2006).
- Song, Y. Y. *et al.* Synthesis and Patterning of Prussian Blue Nanostructures on Silicon Wafer via Galvanic Displacement Reaction. *Adv. Funct. Mater.* **17**, 2808–2814 (2007).
- Ghicov, A. & Schmuki, P. Self-ordering electrochemistry: a review on growth and functionality of  $\text{TiO}_2$  nanotubes and other self-aligned  $\text{MO}_x$  structures. *Chem. Commun.* **20**, 2791–2808 (2009).
- Wang, J. & Lin, Z. Q. Freestanding  $\text{TiO}_2$  Nanotube Arrays with Ultrahigh Aspect Ratio via Electrochemical Anodization. *Chem. Mater.* **20**, 1257–1261 (2008).
- Gao, Z. D., Liu, H. F., Li, C. Y. & Song, Y. Y. Biotemplated Synthesis of Au Nanoparticles- $\text{TiO}_2$  Nanotube Junctions for Enhanced Direct Electrochemistry of Heme Proteins. *Chem. Commun.* **49**, 774–776 (2013).
- Sarauli, D. *et al.* Semimetallic  $\text{TiO}_2$  nanotubes: New interfaces for bioelectrochemical enzymatic catalysis. *J. Mater. Chem.* **22**, 4615–4618 (2012).
- An, Z., Wang, Y. & He, J. Distribution-enhanced direct electron communication of hemoglobin immobilized in pristine  $\text{TiO}_2$  nanotube arrays. *J. Mater. Chem.* **21**, 15780–15787 (2011).
- Wu, F. *et al.* Direct electrochemistry of horseradish peroxidase on  $\text{TiO}_2$  nanotube arrays via seeded-growth synthesis. *Biosens. Bioelectro.* **24**, 198–203 (2008).
- Liu, S. & Chen, A. Coadsorption of horseradish peroxidase with thionine on  $\text{TiO}_2$  nanotubes for biosensing. *Langmuir* **21**, 8409–8413 (2005).
- Tang, H., Prasad, K., Sanjines, R., Schmid, P. E. & Levy, F. Electrical and optical properties of  $\text{TiO}_2$  anatase thin films. *J. Appl. Phys.* **75**, 2042–2047 (1994).
- Homma, T., Sumita, D., Kondo, M., Kuwahara, T. & Shimomura, M. Amperometric glucose sensing with polyaniline/poly(acrylic acid) composite film bearing covalently-immobilized glucose oxidase: A novel method combining enzymatic glucose oxidation and cathodic  $\text{O}_2$  reduction. *J. Electroanal. Chem.* **712**, 119–123 (2014).
- Chauhan, N., Singh, A., Narang, J., Dahiya, S. & Pundir, C. S. Development of amperometric lysine biosensors based on Au nanoparticles/multiwalled carbon nanotubes/polymers modified Au electrodes. *Analyst* **137**, 5113–5122 (2012).
- Xue, M. H., Xu, Q., Zhou, M. & Zhu, J. J. *In situ* immobilization of glucose oxidase in chitosan-gold nanoparticle hybrid film on Prussian Blue modified electrode for high-sensitivity glucose detection. *Electrochem. Commun.* **8**, 1468–1474 (2006).
- Ricci, F., Amine, A., Palleschi, G. & Moscone, D. Prussian blue based screen printed biosensors with improved characteristics of long-term lifetime and pH stability. *Biosens. Bioelectro.* **18**, 165–174 (2003).
- Yu, J. & Zhou, M. Effects of calcination temperature on microstructures and photocatalytic activity of titanate nanotube films prepared by an EPD method. *Nanotechnology* **19**, 045606 (2008).
- Lai, G. S., Yan, F. & Ju, H. X. Dual signal amplification of glucose oxidase-functionalized nanocomposites as a trace label for ultrasensitive simultaneous multiplexed electrochemical detection of tumor markers. *Anal. Chem.* **81**, 9730–9736 (2009).
- Li, J., Qiu, J. D., Xu, J. J., Chen, H. Y. & Xia, X. H. The synergistic effect of Prussian-Blue-grafted carbon nanotube/poly(4-vinylpyridine) composites for amperometric sensing. *Adv. Funct. Mater.* **17**, 1574–1580 (2007).
- Zhu, N., Han, S., Gan, S., Ulstrup, J. & Chi, Q. Graphene Paper Doped with Chemically Compatible Prussian Blue Nanoparticles as Nanohybrid Electrocatalyst. *Adv. Funct. Mater.* **23**, 5297–5306 (2013).
- Raicopol, M., Pruna, A., Damian, C. & Pilan, L. Functionalized single-walled carbon nanotubes/polypyrrole composites for amperometric glucose biosensors. *Nanoscale Res. Lett.* **8**, 316 (2013).
- Safavi, A., Maleki, N. & Farjania, E. Fabrication of a glucose sensor based on a novel nanocomposite electrode. *Biosens. Bioelectro.* **24**, 1655–1660 (2009).
- Shobha Jeykumari, D. R. & Sriman Narayanan, S. Functionalized carbon nanotube-bienzyme biocomposite for amperometric sensing. *Carbon* **47**, 957–966 (2009).
- Zhong, X. *et al.* An Amperometric biosensor for glucose based on self-assembling nanoparticles and electrosynthesis of poly-o-diaminobenzene on the Prussian blue modified gold electrode. *Anal. Lett.* **38**, 1085–1097 (2005).

## Acknowledgments

This work was supported by the National Natural Science Foundation of China (No. 21322504, 21275026, 11174046), the Fundamental Research Funds for the Central Universities (N120505002, N120505006, N110805001), and the Program for Liaoning Excellent Talents in University (LJQ2013028).

## Author contributions

Z.-D.G. and Y.-Y.S. conducted the research and discussed the results. Y.Q. and T.L. prepared the anodized samples. Y.Q. carried out the electrochemical experiments. Z.-D.G., Y.Q. and T.L. carried out the materials characterizations. Z.-D.G. and N.K.S. drafted the paper. All of the authors reviewed the manuscript and participated in discussions on the results of this research.

## Additional information

**Competing financial interests:** The authors declare no competing financial interests.

**How to cite this article:** Gao, Z.-D., Qu, Y., Li, T., Shrestha, N.K. & Song, Y.-Y. Development of Amperometric Glucose Biosensor Based on Prussian Blue Functionalized  $\text{TiO}_2$  Nanotube Arrays. *Sci. Rep.* **4**, 6891; DOI:10.1038/srep06891 (2014).



This work is licensed under a Creative Commons Attribution-NonCommercial-ShareAlike 4.0 International License. The images or other third party material in this article are included in the article's Creative Commons license, unless indicated otherwise in the credit line; if the material is not included under the Creative Commons license, users will need to obtain permission from the license holder in order to reproduce the material. To view a copy of this license, visit <http://creativecommons.org/licenses/by-nc-sa/4.0/>